

From breather solutions to lump solutions: A construction method for the Zakharov equation

Feng Yuan(袁丰), Behzad Ghanbari, Yongshuai Zhang(张永帅), and Abdul Majid Wazwaz
Citation: Chin. Phys. B, 2023, 32 (**12**): 120201. DOI: 10.1088/1674-1056/acf706
Journal homepage: http://cpb.iphy.ac.cn; http://iopscience.iop.org/cpb

What follows is a list of articles you may be interested in

Interaction solutions and localized waves to the (2+1)-dimensional Hirota-Satsuma-Ito equation with variable coefficient

Xinying Yan(闫鑫颖), Jinzhou Liu(刘锦洲), and Xiangpeng Xin(辛祥鹏)
Chin. Phys. B, 2023, 32 (**7**): 070201. DOI: 10.1088/1674-1056/acb9f2

Interaction solutions for the second extended (3+1)-dimensional Jimbo-Miwa equation

Hongcai Ma(马红彩), Xue Mao(毛雪), and Aiping Deng(邓爱平)
Chin. Phys. B, 2023, 32 (**6**): 060201. DOI: 10.1088/1674-1056/acb91c

Superposition formulas of multi-solution to a reduced (3+1)-dimensional nonlinear evolution equation

Hangbing Shao(邵杭兵) and Bilige Sudao(苏道毕力格)
Chin. Phys. B, 2023, 32 (**5**): 050204. DOI: 10.1088/1674-1056/acae7d

Positon and hybrid solutions for the (2+1)-dimensional complex modified Korteweg-de Vries equations

Feng Yuan(袁丰) and Behzad Ghanbari
Chin. Phys. B, 2023, 32 (**4**): 040201. DOI: 10.1088/1674-1056/ac935b

Soliton, breather, and rogue wave solutions for solving the nonlinear Schrödinger equation using a deep learning method with physical constraints

Jun-Cai Pu(蒲俊才), Jun Li(李军), and Yong Chen(陈勇)
Chin. Phys. B, 2021, 30 (**6**): 060202. DOI: 10.1088/1674-1056/abd7e3

From breather solutions to lump solutions: A construction method for the Zakharov equation

Feng Yuan(袁丰)[1,†], Behzad Ghanbari[2], Yongshuai Zhang(张永帅)[3], and Abdul Majid Wazwaz[4]

[1] *College of Science, Nanjing University of Posts and Telecommunications, Nanjing* 210023, *China*
[2] *Department of Mathematics, Kermanshah University of Technology, Kermanshah, Iran*
[3] *Department of Mathematics, Shaoxing University, Shaoxing* 312000, *China*
[4] *Department of Mathematics, Saint Xavier University, Chicago, IL* 60655, *USA*

(Received 16 July 2023; revised manuscript received 23 August 2023; accepted manuscript online 6 September 2023)

Periodic solutions of the Zakharov equation are investigated. By performing the limit operation $\lambda_{2l-1} \to \lambda_1$ on the eigenvalues of the Lax pair obtained from the n-fold Darboux transformation, an order-n breather-positon solution is first obtained from a plane wave seed. It is then proven that an order-n lump solution can be further constructed by taking the limit $\lambda_1 \to \lambda_0$ on the breather-positon solution, because the unique eigenvalue λ_0 associated with the Lax pair eigenfunction $\Psi(\lambda_0) = 0$ corresponds to the limit of the infinite-periodic solutions. A convenient procedure of generating higher-order lump solutions of the Zakharov equation is also investigated based on the idea of the degeneration of double eigenvalues in multi-breather solutions.

Keywords: Zakharov equation, breather solution, b-positon solution, lump solution

PACS: 02.30.Ik, 02.30.Jr, 05.45.–a **DOI:** 10.1088/1674-1056/acf706

1. Introduction

As an important branch of the nonlinear science, the theory of integrable systems has been widely applied to various fields, including mathematics, physics, biology, oceanography, etc. The studies of integrable systems focus on the development of analytical models that have dipicted plenty of natural phenomena as well as precise analyses of complex nonlinear partial differential equations (NPDEs).

For a typical integrable system, the nonlinear Schrödinger (NLS) equation reads

$$\mathrm{i}q_t + q_{xx} + 2\varepsilon q|q|^2 = 0, \quad \varepsilon = \pm 1, \tag{1}$$

which originates from the physics of nonlinear dispersion mediums with a cubic-form nonlinearity term.[1,2]

The NLS equation has been proven to be a fully integrable nonlinear system, which makes it a useful model in many technological applications. For example, it provides guidelines for the generation of solitons in planar waveguides in self-trapped beams[3] and in nonlinear fibers.[4] Theoretically, fruitful analytical solutions of the NLS equation have been proposed.[5–9]

The general statement on nonlinear equations can provide strong theoretical support to our physical and experimental findings. Among all the promotion methodologies, an appropriate one would be multiplying the dimensions of the integrable system. Introducing additional variables is a technique that can increase the spatial dimension of a nonlinear equation without compromising the integrability of the original equation. This is a crucial aspect of research, as it allows for more complex models to be analyzed while retaining the integrability property of the equation. So far, the NLS equation has extended itself to $2+1$ dimensions by several means.

Firstly proposed by Davey and Stewartson in 1974,[10] the Davey–Stewartson (DS) equation is an important $(2+1)$-dimensional generalization of the NLS equation, namely,

$$\begin{aligned} &\mathrm{i}A_t = A_{xx} + A_{yy} + (\varepsilon|A|^2 - 2Q)A, \\ &Q_{xx} - Q_{yy} = (\varepsilon|A|^2)_{xx}, \quad \varepsilon = \pm 1, \end{aligned} \tag{2}$$

where A and Q denote complex and real functions, respectively. The DS equation finds extensive applications in various fields including plasma physics,[11] nonlinear optics,[12] and fluid mechanics.[13] Regarding the analytical solutions of this equation, rogue waves, lump solutions, and hybrid solutions that combine lumps and solitons have been constructed.[14–19]

As another $(2+1)$-dimensions generalization, the Zakharov equation is the main topic of this study, that is,[20]

$$\begin{aligned} &\mathrm{i}q_t + q_{xy} + 2Vq = 0, \\ &V_y = \varepsilon(|q|^2)_x, \quad \varepsilon = \pm 1, \end{aligned} \tag{3}$$

where $q(x, y, t)$ is a complex function and V is a real function. It should be noticed that the Zakharov equation becomes the NLS equation if $\partial_x = \partial_y$. Constructed firstly by Zakharov in 1980,[20] the Zakharov equation has been widely studied due to its physical background. This equation was later re-derived by Strachan from symmetry space-based integrable systems and through the reduction in terms of dimensions on the self-dual Yang–Mills equation.[21,22]

†Corresponding author. E-mail: yf2017@mail.ustc.edu.cn

© 2023 Chinese Physical Society and IOP Publishing Ltd

The Lax pair, Darboux transformation, and Hirota bilinear forms of the Zakharov equation have been presented in Refs. [22–24]. In Ref. [25], the authors studied its geometrical and gauge equivalent counterparts, and in Ref. [26] Velan and Lakshmanan investigated the infinite-dimensional Lie algebras of (3) Lie symmetries. Plenty of analytical solutions have also been discovered, including various solitons,[27–30] Jacobi elliptic function solutions,[31] and line rogue waves.[32–36] In Ref. [37] Radha and Lakshmanan generated a new class of "induced localized structures" by the line soliton's interaction with a curved soliton.

Despite extensive research on the exact solutions of the Zakharov equation, the spatially periodic solutions, including breather solutions, b-position solutions, and lump solutions, have not been well studied. Lumps are 2D soliton solutions that are weakly localized and decay algebraically in all directions.[38–46] They are a type of rational function solutions that are frequently observed in high-dimensional systems. The investigation and examination of lump solutions in high-dimensional systems is an interesting area of research.[43–47]

The primary target of this study is to obtain lump solutions from the breather and b-positon solutions of Eq. (3) when $\varepsilon = 1$. The fundamental method we use is the Darboux transformation. Previous studies have shown that multi-breather solutions associated with the NLS equation can result in higher-order rational solutions.[9] Correspondingly, there remain two main questions:

1. Does an explicit lump solution exist for the Zakharov equation?

2. How can we explain the origins of these solutions?

To obtain the lump solutions of the Zakharov equation, we propose a two-stage eigenvalue degradation process for the multi-breather solutions. In order to carry out this double degradation process on the Lax pair eigenvalue, the b-position solution of the Zakharov equation is first constructed, which can be obtained from the breather solution of the limit $\lambda_{2l-1} \to \lambda_1$.[48–50]

The rest of this paper is organized as follows. In Section 2 we introduce the determinant representation of DT to rephrase the n-soliton solution of the Zakharov equation. In Section 3, the derivation of n-order breather solutions is demonstrated and the general forms of b-positon solution and lump are presented. Moreover, we investigate the double degradation of eigenvalues. In Section 4, we present our conclusion remarks.

2. The n-solutions

First of all, considering $\varepsilon = 1$ in Eq. (3) yields

$$\mathrm{i}q_t + q_{xy} + 2q\int |q|_y^2 \mathrm{d}x = 0. \tag{4}$$

The corresponding Lax pair is

$$\begin{aligned} \Psi_x &= M\Psi, \\ \Psi_t &= 2\lambda\Psi_y + N\Psi, \end{aligned} \tag{5}$$

with

$$\Psi = \begin{bmatrix} \psi_1(\lambda, x, y, t) \\ \psi_2(\lambda, x, y, t) \end{bmatrix}, \quad M = \begin{bmatrix} -\mathrm{i}\lambda & q \\ -q^* & \mathrm{i}\lambda \end{bmatrix},$$
$$N = \begin{bmatrix} \mathrm{i}\int |q|_y^2 \mathrm{d}x & \mathrm{i}q_y \\ \mathrm{i}q_y^* & -\mathrm{i}\int |q|_y^2 \mathrm{d}x \end{bmatrix}.$$

Here $\lambda \in \mathbb{C}$, λ is the eigenvalue of Eq. (5), and * denotes the conjugation operator. The Darboux transformation and n-solution have been given in Ref. [29]. The n-solution can be rewritten as

$$q^{[n]} = q^{[0]} + 2\mathrm{i}\frac{D_{2n}}{W_{2n}}, \tag{6}$$

with

$$D_{2n} = \begin{vmatrix} \psi_{11} & \psi_{12} & \lambda_1\psi_{11} & \lambda_1\psi_{12} & \dots & \lambda_1^{n-2}\psi_{12} & \lambda_1^{n-1}\psi_{11} & \lambda_1^{n}\psi_{11} \\ \psi_{21} & \psi_{22} & \lambda_2\psi_{21} & \lambda_2\psi_{22} & \dots & \lambda_1^{n-2}\psi_{22} & \lambda_2^{n-1}\psi_{21} & \lambda_2^{n}\psi_{21} \\ \vdots & \vdots & \vdots & \vdots & \ddots & \vdots & \vdots & \vdots \\ \psi_{2n,1} & \psi_{2n,2} & \lambda_{2n}\psi_{2n,1} & \lambda_{2n}\psi_{2n,2} & \dots & \lambda_1^{n-2}\psi_{2n,2} & \lambda_{2n}^{n-1}\psi_{2n,1} & \lambda_{2n}^{n}\psi_{2n,1} \end{vmatrix},$$

$$W_{2n} = \begin{vmatrix} \psi_{11} & \psi_{12} & \lambda_1\psi_{11} & \lambda_1\psi_{12} & \dots & \lambda_1^{n-1}\psi_{11} & \lambda_1^{n-1}\psi_{12} \\ \psi_{21} & \psi_{22} & \lambda_2\psi_{21} & \lambda_2\psi_{22} & \dots & \lambda_2^{n-1}\psi_{21} & \lambda_2^{n-1}\psi_{22} \\ \vdots & \vdots & \vdots & \vdots & \ddots & \vdots & \vdots \\ \psi_{2n,1} & \psi_{2n,2} & \lambda_{2n}\psi_{2n,1} & \lambda_{2n}\psi_{2n,2} & \dots & \lambda_{2n}^{n-1}\psi_{2n,1} & \lambda_{2n}^{n-1}\psi_{2n,2} \end{vmatrix}.$$

Here, λ_{2k-1} and $\lambda_{2k}\,(k = 1, \dots, n)$ are n sets of eigenvalues corresponding to Lax pair, and $\lambda_{2k-1} = \lambda_{2k}^*$, $\psi_{2k-1,1} = \psi_{2k,2}^*$, $\psi_{2k-1,2} = -\psi_{2k,1}^*$.

3. The breather, b-positon, and lump solutions

By solving Eq. (5) using the initial plane wave seed $q = c\,\mathrm{e}^{\mathrm{i}\rho}$ (where a, b, and c are real constants and $\rho = ax + by - abt$, a, b, c), one can derive a total of n sets of eigen-

values and their corresponding eigenfunctions as follows:

$$\begin{aligned}
\psi_{2k-1,1} &= \mathrm{e}^{\frac{\mathrm{i}\rho}{2}}\left(c\,\mathrm{e}^{\mathrm{i}\eta_{2k-1}}+\frac{\mathrm{i}}{2}(a+2\lambda_{2k-1}+s_{2k-1})\,\mathrm{e}^{-\mathrm{i}\eta_{2k-1}}\right),\\
\psi_{2k-1,2} &= \mathrm{e}^{-\frac{\mathrm{i}\rho}{2}}\left(c\,\mathrm{e}^{-\mathrm{i}\eta_{2k-1}}+\frac{\mathrm{i}}{2}(a+2\lambda_{2k-1}+s_{2k-1})\,\mathrm{e}^{\mathrm{i}\eta_{2k-1}}\right),\\
\psi_{2k,1} &= -\mathrm{e}^{-\frac{\mathrm{i}\rho}{2}}\left(c\,\mathrm{e}^{\mathrm{i}\eta_{2k}}-\frac{\mathrm{i}}{2}(a+2\lambda_{2k}+s_{2k})\,\mathrm{e}^{-\mathrm{i}\eta_{2k}}\right),\\
\psi_{2k,2} &= \mathrm{e}^{-\frac{\mathrm{i}\rho}{2}}\left(c\,\mathrm{e}^{-\mathrm{i}\eta_{2k}}-\frac{\mathrm{i}}{2}(a+2\lambda_{2k}+s_{2k})\,\mathrm{e}^{\mathrm{i}\eta_{2k}}\right).
\end{aligned}\tag{7}$$

In Eq. (7), we set $\eta_k=\frac{s_k}{2}(x+2\alpha\lambda_k y-(b-4\alpha\lambda_k^2)t)$, $s_k=\sqrt{4c^2+(a+2\lambda_k)^2}$, $\alpha\neq 0$.

To obtain the order-n breather solution, we can substitute Eq. (7) and the seed solution $q^{[0]}=c\,\mathrm{e}^{\mathrm{i}\rho}$ into Eq. (6). Without loss of generality, we can assume $\lambda_{2k-1}=-\frac{a}{2}+\beta_k\mathrm{i}$, where $c>0$, $\beta_k>0$, and $c\neq\beta_k$. Under these conditions, the order-1 breather solution can be simplified to

$$|q_b^{[1]}|^2=\frac{\beta_1^2c^2\cos^2\theta_1-2\beta_1c(2\beta_1^2-c^2)\cos\theta_1\cosh\theta_2+c^4\cosh^2\theta_2+4\beta_1^2(\beta_1^2-c^2)}{(c\cosh\theta_2-\beta_1\cos\theta_1)^2},\tag{8}$$

where $\theta_1=2\sqrt{c^2-\beta_1^2}(x-a\alpha y-(b-a^2\alpha-4\alpha\beta_1^2)t)$, $\theta_2=4\alpha\beta_1\sqrt{c^2-\beta_1^2}(y-2at)$.

The coordinates of crests and valleys can be obtained by solving $\partial|q^{[1]}|/\partial x=0$ and $\partial|q^{[1]}|/\partial y=0$. Depending on the selected parameters, three different scenarios can be observed.

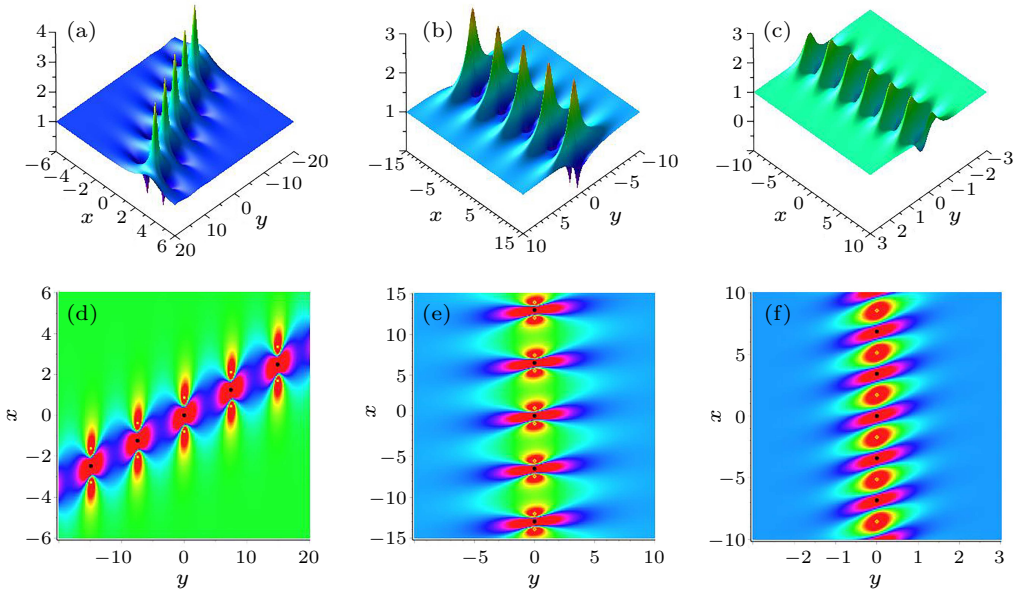


Fig. 1. Behavior of $|q_b^{[1]}|$ for $a=1/2$, $b=1$, $c=1$, $t=0$: (a) $\alpha=1/3$, $\beta_1=8/7$, (b) $\alpha=1/3$, $\beta_1=7/8$, (c) $\alpha=2$, $\beta_1=2/5$. (a)–(c) Three-dimensional profiles. (d)–(f) Their corresponding density profiles. The black points are the position of the crests, and the yellow points are the position of the valleys.

(I) When $0<c<\beta_1$, the coordinates of the crests on the (x,y)-plane can be expressed as

$$\left[(\alpha a^2+4\alpha\beta_1^2+b)t\pm\frac{am\pi}{2\beta_1\sqrt{\beta_1^2-c^2}},\,2at\pm\frac{m\pi}{2\alpha\beta_1\sqrt{\beta_1^2-c^2}}\right],$$

where m is an integer. Additionally, the valleys can be found at $([a^2\alpha+4\alpha\beta_1^2+b]t\pm\frac{1}{2\sqrt{\beta_1^2-c^2}}\ln[\frac{2\beta_1^2-c^2+\sqrt{4\beta_1^4-5\beta_1^2c^2+c^4}}{\beta_1 c}]\pm\frac{am\pi}{2\beta_1\sqrt{\beta_1^2-c^2}},\,2at\pm\frac{m\pi}{2\alpha\beta_1\sqrt{\beta_1^2-c^2}})$. As illustrated in Figs. 1(a) and 1(d), the order-1 breather comprises of one peak and two valleys.

(II) When $\beta_1<c<2\beta_1$, the coordinates of the crests on the (x,y) plane can be expressed as

$$\left([\alpha a^2+4\alpha\beta_1^2+b]t\pm\frac{m\pi}{\sqrt{c^2-\beta_1^2}},\,2at\right),$$

where m is an integer. Additionally, the valleys can be found at

$$\left([\alpha a^2+4\alpha\beta_1^2+b]t-\frac{\arccos[\frac{2\beta_1}{c}\pm\frac{c}{\beta_1}]\pm 2m\pi}{2\sqrt{c^2-\beta_1^2}},\,2at\right).$$

Figures 1(b) and 1(e) display the one peak and two valleys present in each unit of the order-1 breather.

(III) When $c\geqslant 2\beta_1$, the coordinates of the crests on the (x,y) plane can be expressed as

$$\left([\alpha a^2+4\alpha\beta_1^2+b]t\pm\frac{m\pi}{\sqrt{c^2-\beta_1^2}},\,2at\right),$$

where m is an integer. Additionally, the valleys can be found

at

$$\left([\alpha a^2+4\alpha\beta_1^2+b]t+\frac{\pi\pm 2m\pi}{2\sqrt{c^2-\beta_1^2}},\ 2at\right).$$

As depicted in Figs. 1(c) and 1(f), the order-1 breather consists of one peak and one valley in each unit.

It can be deduced easily that the maximal amplitude of $|q_b^{[1]}|$ is equal to $2\beta_1+c$. The velocity in the (x,y) direction of $|q_b^{[1]}|$ is given by $(\alpha a^2+4\alpha\beta_1^2+b,\ 2a)$. This implies that if $a=0$, the breather will only move along the x direction. When $c<2\beta_1$, the minimal amplitude of $|q_b^{[1]}|$ is 0. However, if $c\geqslant 2\beta_1$, the minimal amplitude is $c-2\beta_1$. The distance between the two peaks is $\frac{\pi}{\sqrt{c^2-\beta_1^2}}$ when $c>\beta_1$, and it is $\frac{\pi\sqrt{a^2\alpha^2+1}}{2\alpha\beta_1\sqrt{\beta_1^2-c^2}}$ when $c<\beta_1$. In the case of $c<\beta_1$, the line where the crest is located is $x-a\alpha y+a\alpha(\alpha a^2-4\alpha\beta_1^2-b)t=0$, while it is $y=2at$ when $c>\beta_1$. The peaks and valleys are illustrated in Fig. 1.

By setting the limit of λ_{2l-1} toward to $\lambda_1=-\frac{a}{2}+\beta_1\mathrm{i}$, one can form order-$n$ b-positon solutions using order-n breather solutions.

Theorem 1 The order-n b-positon solution for the Zakharov equation is

$$q_{bp}^{[n]}=c\mathrm{e}^{\mathrm{i}\rho}-2\mathrm{i}\frac{\Delta_1}{\Delta_2},\tag{9}$$

with

$$\Delta_1=\left(\frac{\partial^{n_j}}{\partial\varepsilon^{n_j}}\Big|_{\varepsilon=0}(D_{2n})_{jk}(\lambda_j+\varepsilon)\right)_{2n\times 2n},\quad \lambda_{2l-1}=\lambda_1,$$
$$\Delta_2=\left(\frac{\partial^{n_j}}{\partial\varepsilon^{n_j}}\Big|_{\varepsilon=0}(W_{2n})_{jk}(\lambda_j+\varepsilon)\right)_{2n\times 2n},\quad n_j=\left[\frac{j-1}{2}\right],$$

where $[\ ]$ means taking the integer part. D_{2n} and W_{2n} are given in Eq. (6) and ψ_{jk} are given in Eq. (7).

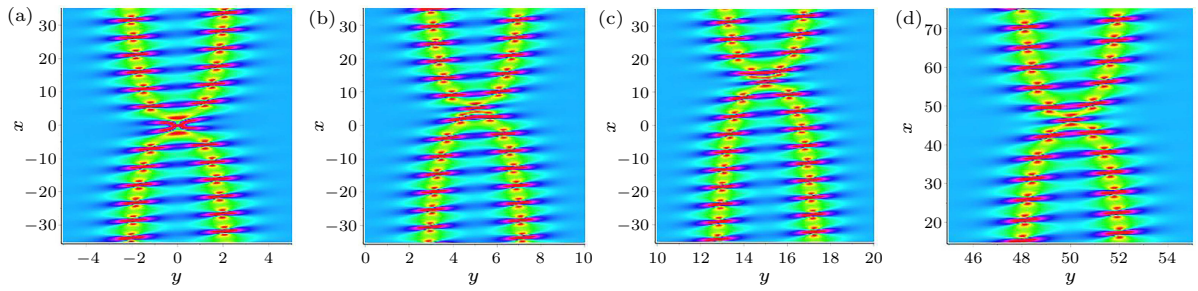


Fig. 2. Density of $|q_{bp}^{[2]}|$ with $a=1/2$, $b=1$, $c=1$, $\alpha=1$, $\beta_1=4/5$: (a) $t=0$, (b) $t=5$, (c) $t=15$, (d) $t=50$.

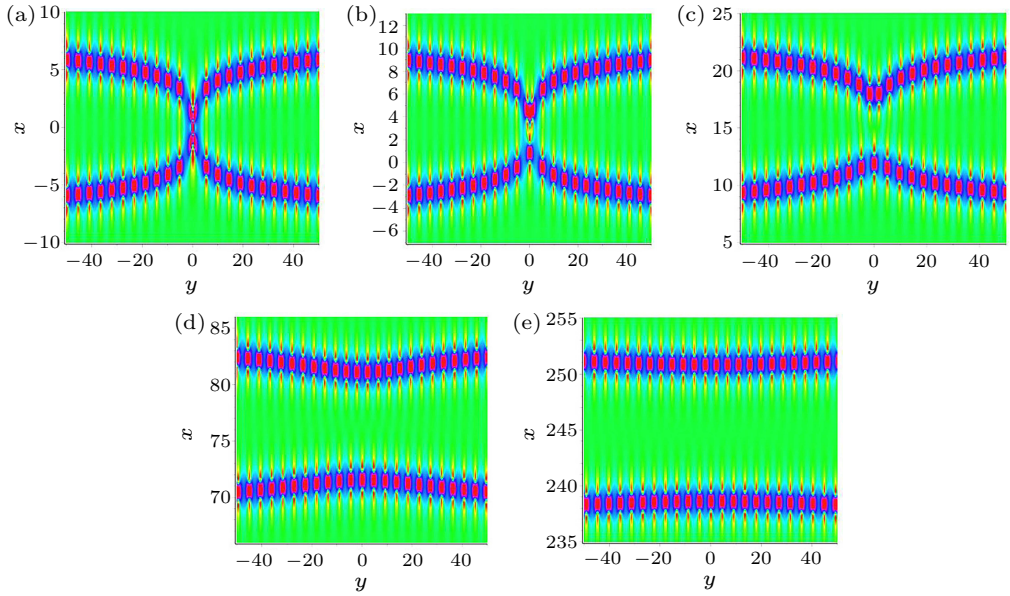


Fig. 3. Density of $|q_{bp}^{[2]}|$ with $a=0$, $b=1/2$, $c=2/3$, $\alpha=1$, $\beta_1=4/5$: (a) $t=0$, (b) $t=1$, (c) $t=5$, (d) $t=25$, (e) $t=80$.

Finding an order-1 b-positon, simply a single breather, is trivial. The next nontrivial solution is an order-2 b-positon with a phase difference between the trajectories of the high-order b-positon and the order-1 breather solution, similar to Refs. [9,49,50]. An order-n b-positon exhibits n parallel breathers of the same shape, making its dynamics comparable to the interaction between order-n breathers. In this context, we focus on the order-2 case. To obtain the order-2 b-positon solution, we set $n=2$ in Eq. (9). Figures 2 and 3 depict the dynamics of the order-2 b-positon solution with varying parame-

ters. If $c>\beta_1$, the interaction between two units of the order-2 b-positon is perpetual, as illustrated in Fig. 2. Conversely, if $c<\beta_1$, the interaction between two breathers is strongest at $t=0$ and gradually diminishes over time. For $t\to\infty$, the order-2 b-positon displays two parallel breathers of the same shape, as shown in Fig. 3. The first nontrivial degenerate breather is the order-2 degenerate breather, which is given as follows:

$$q_{bp}^{[2]}=\mathrm{e}^{\mathrm{i}\rho}\left(c-2\mathrm{i}\frac{\Theta_1}{\Theta_2}\right), \tag{10}$$

where

$$\begin{aligned}\Theta_1=&4\mathrm{i}\beta_1 g_1 g_2^*(g_1 g_1^*-g_2 g_2^*)-4a\beta_1 g_2^* g_4^*(g_1 g_4-g_2 g_3)\\&+4\beta_1^2[g_1^2(g_1^* g_4^*-g_2^* g_3^*)+g_2^{*2}(g_1 g_4-g_2 g_3)]\\&-2\mathrm{i}a\beta_1[g_1 g_2^*(g_1 g_3^*+g_2 g_4^*)+g_2^*(g_1 g_4-g_2 g_3)],\\ \Theta_2=&4\beta_1^2(g_1 g_1^* g_4 g_4^*+g_2 g_2^* g_3 g_3^*-g_1 g_2 g_4 g_3^*-g_2 g_1^* g_3 g_4^*)\\&+(g_1 g_1^*+g_2 g_2^*)^2,\end{aligned}$$

$$\begin{aligned}g_1=&c\,\mathrm{e}^{\xi_1}+(\mathrm{i}\sqrt{c^2-\beta_1^2}-\beta_1)\,\mathrm{e}^{-\xi_1},\\ g_2=&(\mathrm{i}\sqrt{c^2-\beta_1^2}-\beta_1)\,\mathrm{e}^{\xi_1}+c\,\mathrm{e}^{-\xi_1},\\ g_3=&\frac{(\xi_2+1)(\mathrm{i}\sqrt{c^2-\beta_1^2}-\beta_1)\,\mathrm{e}^{-\xi_1}-c\xi_2\,\mathrm{e}^{\xi_1}}{\sqrt{c^2-\beta_1^2}},\\ g_4=&\frac{(\xi_2-1)(\mathrm{i}\sqrt{c^2-\beta_1^2}-\beta_1)\,\mathrm{e}^{\xi_1}+c\xi_2\,\mathrm{e}^{-\xi_1}}{\sqrt{c^2-\beta_1^2}},\\ \xi_1=&\mathrm{i}\sqrt{c^2-\beta_1^2}\Big(x-bt-\alpha(a-2\mathrm{i}\beta_1)(y-(a-2\mathrm{i}\beta_1)^2t)\Big),\\ \xi_2=&\beta_1[x-bt-a\alpha y-\alpha(a^2-8c^2+12\beta_1^2)t]\\&-2\mathrm{i}\alpha(c^2-2\beta_1^2)(y-2at).\end{aligned}$$

Through the limits $\lambda_{2l-1}\to\lambda_0=-\frac{a}{2}+\mathrm{i}c$, the order-$n$ lump solutions can be constructed based on the order-n breather solutions.

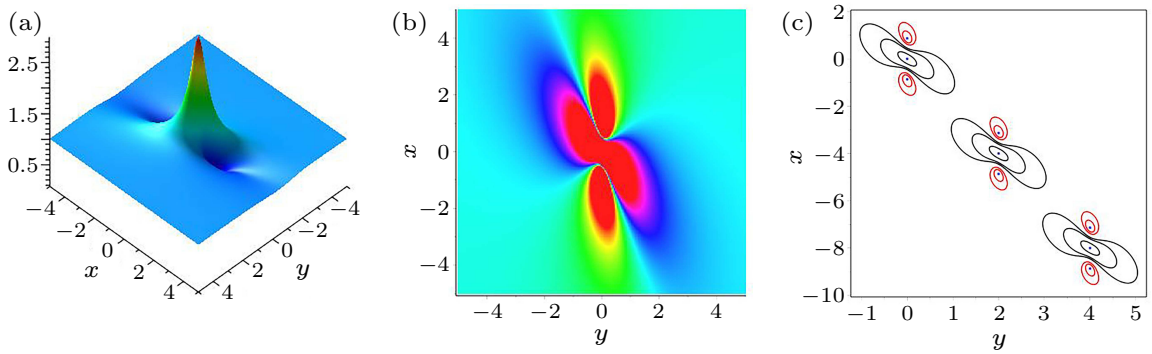


Fig. 4. Characteristics of $|q_{\mathrm{lump}}^{[1]}|$ with $a=1$, $b=1$, $c=1$, $\alpha=-1$: (a) 3D profile, (b) the corresponding density, (c) the contour curves at $t=0$, $t=1$, $t=2$. The black points are the position of the crests and peaks.

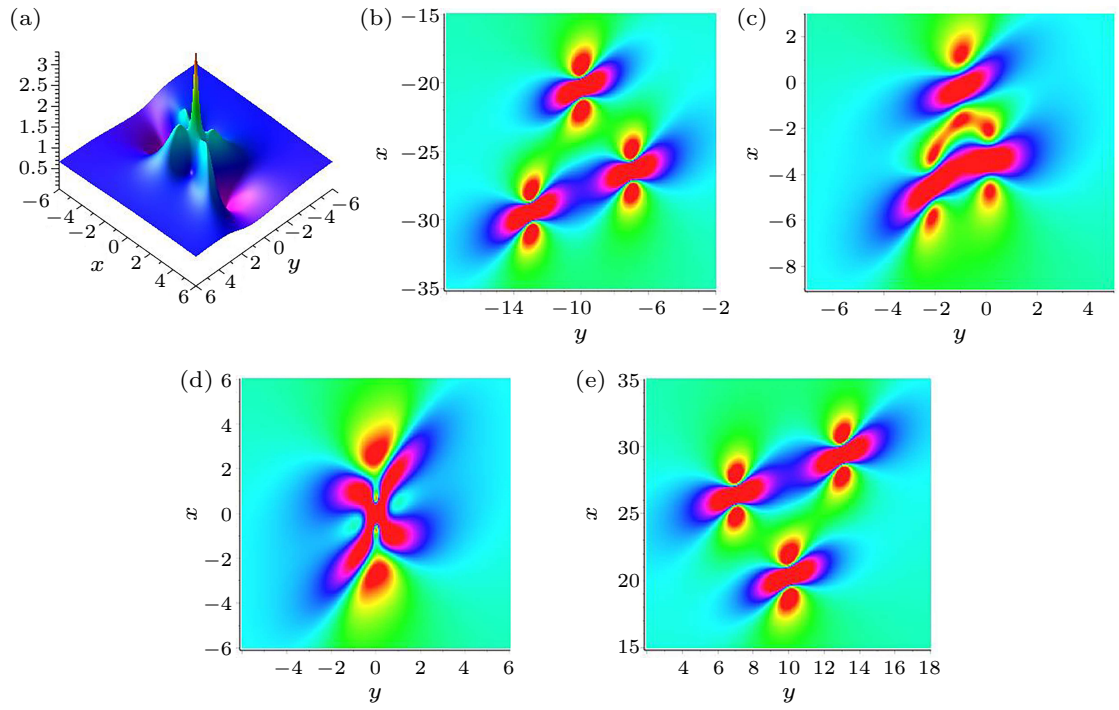


Fig. 5. Density of $|q_{\mathrm{lump}}^{[2]}|$ with $a=1/2$, $b=1/2$, $c=2/3$, $\alpha=1$: (a) $t=0$, (b) $t=-10$, (c) $t=-1$, (d) $t=0$, (e) $t=10$,

Theorem 2 The order-n lump solution for the Zakharov equation is

$$q_{\text{lump}}^{[n]} = c\mathrm{e}^{\mathrm{i}\rho} - 2\mathrm{i}\frac{\Delta_3}{\Delta_4}, \tag{11}$$

with

$$\Delta_3 = \left(\frac{\partial^{n_j}}{\partial\varepsilon^{n_j}}\Big|_{\varepsilon=0}(D_{2n})_{jk}(\lambda_j+\varepsilon)\right)_{2n\times 2n},\ \ \lambda_{2l-1}=\lambda_0,$$
$$\Delta_4 = \left(\frac{\partial^{n_j}}{\partial\varepsilon^{n_j}}\Big|_{\varepsilon=0}(W_{2n})_{jk}(\lambda_j+\varepsilon)\right)_{2n\times 2n},\ \ n_j=\left[\frac{j+1}{2}\right],$$

where $[\ ]$ also means taking the integer part. D_{2n} and W_{2n} are given in Eq. (6) and ψ_{jk} are given in Eq. (7).

Substituting $n=1$ into Eq. (11), the order-1lump solution can be simplified to

$$|q_{\text{lump}}^{[1]}| = \frac{c\sqrt{(8c^4(\theta_2^2+\theta_1^2)-24c^2\theta_2+9)}}{4c^2\theta_2+1}, \tag{12}$$

where $\theta_1 = 16\alpha c^2(y-2at)$, $\theta_2 = \alpha^2(a^2+4c^2)(y-2at)t + 2\alpha(a^2-4c^2)(x-bt)t+(x-bt)^2+\alpha^2(a^2+4c^2)t^2-2a\alpha y(x-bt)$. Its 3D profile and density contour are shown in Figs. 4(a) and 4(b). The lump reaches the maximum $3c$ at the point $[(a^2\alpha+4\alpha c^2+b)t, 2at]$, while it reaches the minimum 0 at the points $[(a^2\alpha+4\alpha c^2+b)t\pm\frac{\sqrt{3}}{2c}, 2at]$. Obviously, the lump translates on the (x,y) plane with a velocity of $(a^2\alpha+4\alpha c^2+b, 2a)$. The dynamics of the order-1 lump is shown in Fig. 4(c). Substituting $n=2$ into Eq. (11), the order-2 lump solution can be obtained. The evolution of the order-2 lump over time can be regarded as the interaction of three order-1 lumps. The three units move on the (x,y) plane and get closer and closer. They fuse at $t=0$ and gradually separate over time. This process is shown in Fig. 5.

According to Ref. [9], transition from an order-n breather to an order-n b-positon to an order-n lump involves a double degradation process. Figures 6 and 7 display the degradation process from an order-2 breather solution to an order-2 lump solution. To emphasize the limit process of $\lambda_3\to\lambda_1$, $\lambda_1\to\lambda_0$, we keep the parameters fixed except for β_j. As $\beta_2\to\beta_1$, the interaction between two units of the order-2 breather gradually weakens, as depicted in Figs. 6(a)–6(d). The order-2 b-positon solution is shown in Fig. 6(e), which resembles Fig. 6(d). As $\beta_1\to c$, the adjacent peaks of the order-2 b-positon move farther apart, as illustrated in Figs. 7(a)–7(d). The topography of Fig. 7(d) is displayed in Fig. 7(e), while Fig. 7(f) depicts an order-2 lump solution. Comparing Fig. 7(e) with Fig. 7(f) confirms that the b-positon's center approximates a lump. Figure 8 shows the sectional views of the order-2 b-positon and lump at $y=0$ corresponding to Figs. 7(e) and 7(f). We can calculate that the coordinates of the points in the graph are approximately $x_{G,H}\approx\pm0.465$ and $x_{E,F}\approx\pm1.757$, while $x_{C,D}\approx\pm0.4649724466$ and $x_{A,B}\approx\pm1.757053408$. In addition, the maximal amplitude of $|q_{bp}^{[2]}|$ is $c+4\beta_1$ and the maximal amplitude of $|q_{\text{lump}}^{[2]}|$ is $5c$. These also verify that the central region of order-2 b-positon is a good approximation of order-2 lump when $\beta_1\approx c$.

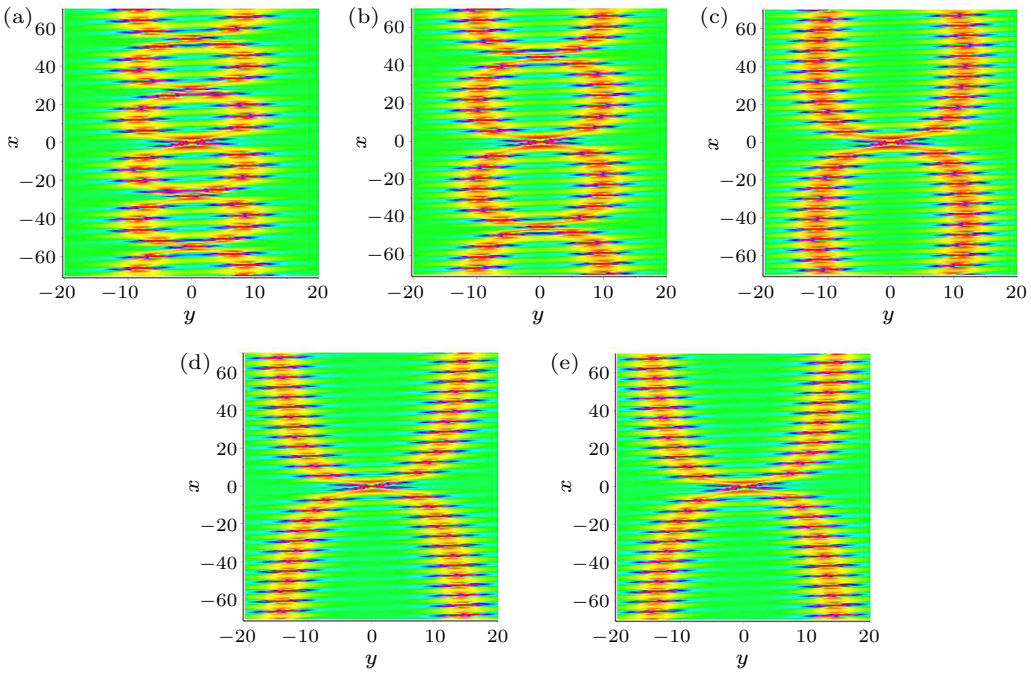


Fig. 6. Density with $a=2/3$, $b=3/4$, $c=1$, $\alpha=1/6$, $t=0$: (a) $|q_b^{[2]}|^2$ for $\beta_1=4/5$, $\beta_2=7/8$, (b) $|q_b^{[2]}|^2$ for $\beta_1=4/5$, $\beta_2=39/46$, (c) $|q_b^{[2]}|^2$ for $\beta_1=4/5$, $\beta_2=19/23$, (d) $|q_b^{[2]}|^2$ for $\beta_1=4/5$, $\beta_2=801/1000$, (e) $|q_{bp}^{[2]}|^2$ for $\beta_1=4/5$.

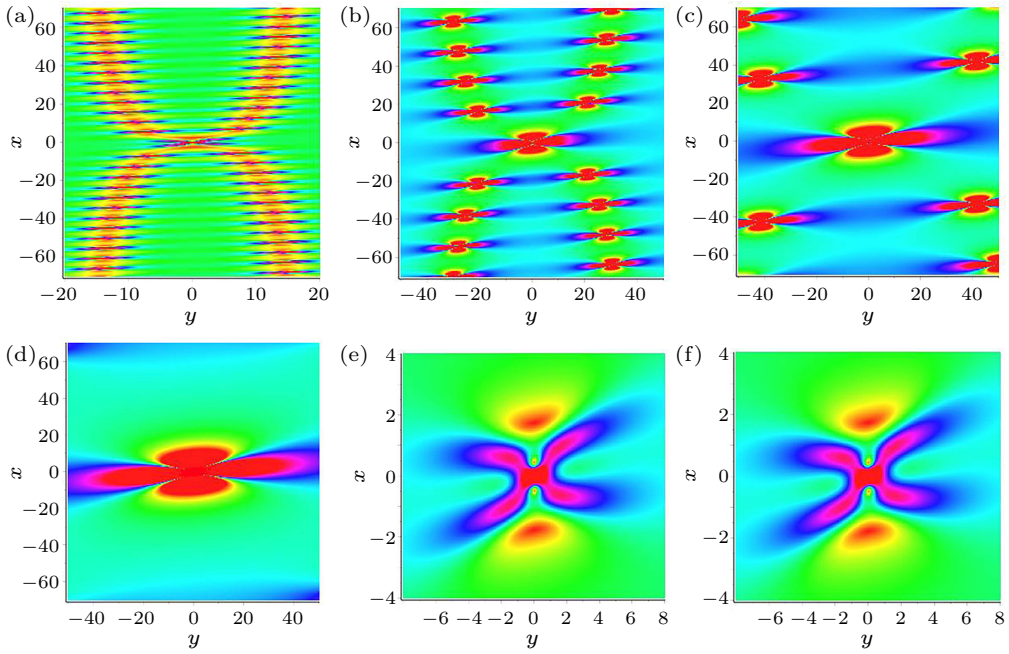


Fig. 7. Density profiles with $a = 2/3$, $b = 3/4$, $c = 1$, $\alpha = 1/6$, $t = 0$: (a) $|q_{bp}^{[2]}|^2$ for $\beta_1 = 49/50$, (b) $|q_{bp}^{[2]}|^2$ for $\beta_1 = 199/200$, (c) $|q_{bp}^{[2]}|^2$ for $\beta_1 = 799/800$, (d)–(f) $|q_{bp}^{[2]}|^2$ for $\beta_1 = 799/800$.

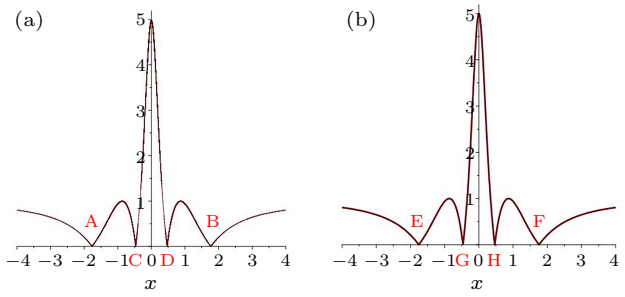


Fig. 8. (a) Sectional view of $|q_{bp}^{[2]}|$ at $y = 0$ with $a = 2/3$, $b = 3/4$, $c = 1$, $\alpha = 1/6$, $\beta_1 = 799/800$, $t = 0$. (b) Sectional view of $|q_{\text{lump}}^{[2]}|$ at $y = 0$ with $a = 2/3$, $b = 3/4$, $c = 1$, $\alpha = 1/6$, $t = 0$.

4. Conclusions

We have systematically provided the order-n breather solutions for the Zakharov equation using the determinant representation of the Darboux transformation described by Eqs. (6) and (7). The formula for the order-1 breather solution is given in Eq. (8), with detailed discussions on the parameter selection of c and β_k in three cases. Additionally, we introduce a new type of periodic solution called the b-positon solution, which is obtained by taking the limit $\lambda_{2l-1} \to \lambda_1$ of the eigenvalues of the Lax pair. This solution is generated from a plane wave seed solution using an n-fold Darboux transformation generated from the order-n breather solution. A formula for the b-positon solution is derived in Eq. (9), utilizing the determinant representation of the higher-order Taylor expansion and the Darboux transformation. Furthermore, the order-n b-positon solution can be transformed into an order-n lump solution via the limiting process on $\lambda_1 \to \lambda_0$, where λ_0 refers to a particular eigenvalue associated with the Lax pair eigenfunction ψ of the Zakharov equation. The formula for the order-1 lump solution is given in Eq. (12), and this study includes the evolutions of the order-1 and order-2 lump solutions over time, as shown in Figs. 4 and 5, respectively. Also we use the derived analytics to illustrate the transition dynamics from the breather to the b-positon solution at an order-2 basis in Fig. 6. This is followed by the transition of the b-positon solution to the lump solution at order-2 basis, as depicted in Fig. 7. In conclusion, this study systematically presents a generation mechanism for higher-order lump solutions of the Zakharov equation from a degeneration process of the dual eigenvalue regarding multi-breather solutions. Our analytical results show the effective mechanism of generating lump solutions of the Zakharov equation from the double eigenvalue degeneration process of breather solutions.

Acknowledgments

This work is sponsored by NUPTSF (Grant Nos. NY220161 and NY222169), the Foundation of Jiangsu Provincial Double-Innovation Doctor Program (Grant No. JSSCBS20210541), the Natural Science Foundation of the Higher Education Institutions of Jiangsu Province (Grant No. 22KJB110004), and the National Natural Science Foundation of China (Grant No. 12171433).

References

[1] Hasegawa A and Tappert F 1972 *Appl. Phys. Lett.* **23** 142
[2] Hasegawa A and Tappert F 1973 *Appl. Phys. Lett.* **23** 171
[3] Maneuf S, Desailly R and Froehly C 1988 *Opt. Commun.* **65** 193
[4] Mollenauer L F, Stolen R H and Gordon J P 1980 *Phys. Rev. Lett.* **45** 1095

[5] Kedziora D J, Ankiewicz A and Akhmediev N 2011 *Phys. Rev. E* **84** 056611
[6] Guo B L, Ling L M and Liu Q P 2012 *Phys. Rev. E* **85** 026607
[7] Ohta Y and Yang J K 2012 *Proc. R. Soc. A* **468** 1716
[8] Kedziora D J, Ankiewicz A and Akhmediev N 2013 *Phys. Rev. E* **88** 013207
[9] Wang L H, He J S, *et al.* 2017 *Phys. Rev. E* **95** 042217
[10] Davey A and Stewartson K 1974 *Proc. R Soc. Lond. A* **338** 101
[11] Panguetna C S, Tabi C B and Kofané T C 2017 *Phys. Plasmas* **24** 092114
[12] Leblond H 2005 *Phys. Rev. Lett.* **95** 033902
[13] Ablowitz M J and Segur H 1979 *J. Fluid Mech.* **92** 691
[14] Fokas A S and Santini P M 1989 *Phys. Rev. Lett.* **63** 1329
[15] Ohta Y and Yang J K 2012 *Phys. Rev. E* **86** 036604
[16] Rao J G, Fokas A S and He J S 2021 *J. Nonlinear Sci.* **31** 67
[17] Guo L J, He J S, Wang L H, *et al.* 2020 *Phys. Rev. Res.* **2** 033376
[18] Guo L J, Chen L, Mihalache D and He J S 2022 *Phys. Rev. E* **105** 014218
[19] Guo L J, Keverkidis P G and He J S 2022 *J. Phys. A: Math. Theo.* **55** 475701
[20] Zakharov V E 1980 *The Inverse Scattering Method.* In: Bullough R K and Caudrey P J (eds) *Solitons. Topics in Current Physics* (Berlin: Springer) Vol. 17 pp 243–285
[21] Strachan I A B 1992 *J. Math. Phys.* **33** 2477
[22] Strachan I A B 1993 *J. Math. Phys.* **34** 243
[23] Radha R and Lakshmanan M 1994 *Inverse Problems* **10** L29
[24] Estevez P G and Hernáez G A 1999 arXiv: solv-int/9910005v1
[25] Myrzakulov R, Vijayalakshmi S, *et al.* 1997 *Phys. Lett. A* **233** 391
[26] Velan M S and Lakshmanan M 1998 *J. Nonlinear Math. Phys.* **5** 190
[27] Strachan I A B 1992 *Inverse Problems* **8** L21
[28] Hosseini K, Sadri K, Salahshour S, *et al.* 2021 *Optik* **229** 166247
[29] Zhang H Q, Li L L and Xue Y S 2009 *Physica A* **388** 9
[30] Yuan F 2022 *Roman. Rep. Phys.* **74** 121
[31] Younis M, Cheemaa N, Mehmood S A, *et al.* 2020 *Waves in Random and Complex Media* **30** 490
[32] Liu C F and Wang Z P 2015 *Int. J. Numer. Methods Heat Fluid Flow* **25** 656
[33] Liu C F, Chen M, Zhou P and Chen L W 2016 *J. Appl. Anal. Comput.* **6** 367
[34] Rao J G, Wang L H, Liu W, *et al.* 2017 *Theor. Math. Phys.* **193** 1783
[35] Wang X B, Tian S F and Zhang T T 2018 *Proc. Am. Math. Soc.* **146** 3353
[36] Chen Y, Wang X B and Han B 2020 *Mod. Phys. Lett. B* **34** 2050234
[37] Radha R and Lakshmanan M 1997 *J. Phys. A: Math. Gen.* **30** 3229
[38] Petviashvili V I 1976 *Plasma Phys.* **2** 469
[39] Ablowitz M J and Satsuma J 1978 *J. Math. Phys.* **19** 2180
[40] Villarroel J and Ablowitz M J 1999 *Commun. Math. Phys.* **207** 1
[41] Jorge M C M, Pacheco G C, *et al.* 2005 *Chaos* **15** 037104
[42] Ma W X 2015 *Phys. Lett. A* **379** 1975
[43] Wang H 2018 *Appl. Math. Lett.* **85** 27
[44] Ma W X and Zhou Y 2018 *J. Different. Equ.* **264** 2633
[45] Rao J G, He J S and Malomed B A 2022 *J. Math. Phys.* **63** 013510
[46] Stepanyants Y, Zakharov D and Zakharov V 2022 *Radiophys. Quantum Electron.* **64** 665
[47] Guo L J, Wang L H, Chen L and He J S 2023 *Stud. Appl. Math.* **151** 35
[48] Xing Q X, Wang L H, Mihalache D, Porsezian K and He J S 2017 *Chaos* **27** 053102
[49] Qiu D Q and Cheng W G 2019 *Appl. Math. Lett.* **98** 13
[50] Yuan F 2021 *Int. J. Mod. Phys. B* **35** 2150053